



Published in final edited form as:

*Mol Pharm.* 2012 November 5; 9(11): 3012–3022. doi:10.1021/mp3004379.

## Aerosolized Antimicrobial Agents Based on Degradable Dextran Nanoparticles Loaded with Silver Carbene Complexes

Cátia Ornelas-Megiatto<sup>†,§</sup>, Parth N. Shah<sup>†,§</sup>, Peter R. Wich<sup>†</sup>, Jessica L. Cohen<sup>†</sup>, Jasur A. Tagaev<sup>‡</sup>, Justin A. Smolen<sup>‡</sup>, Brian D. Wright<sup>¶</sup>, Matthew J. Panzner<sup>¶</sup>, Wiley J. Youngs<sup>¶</sup>, Jean M. J. Fréchet<sup>†,#,\*,</sup>, and Carolyn L. Cannon<sup>†,\*</sup>

<sup>†</sup>College of Chemistry, University of California, Berkeley, California 94720-1460, USA

<sup>‡</sup>Division of Pulmonary and Vascular Biology, Department of Pediatrics, UT Southwestern Medical Center, Dallas, Texas 75390-9063, USA

<sup>¶</sup>Department of Chemistry, University of Akron, Akron, Ohio 44325-0002, USA

<sup>#</sup>King Abdullah University of Science and Technology, Thuwal, 23955-6900, Saudi Arabia

### Abstract

Degradable acetalated dextran (Ac-DEX) nanoparticles were prepared and loaded with a hydrophobic silver carbene complex (SCC) by a single-emulsion process. The resulting particles were characterized for morphology and size distribution using scanning electron microscopy (SEM), transmission electron microscopy (TEM), and dynamic light scattering (DLS). The average particle size and particle size distribution were found to be a function of the ratio of the organic phase to the surfactant containing aqueous phase with a 1:5 volume ratio of Ac-DEX CH<sub>2</sub>Cl<sub>2</sub> (organic): PBS (aqueous) being optimal for the formulation of nanoparticles with an average size of 100 ± 40 nm and a low polydispersity. The SCC loading was found to increase with an increase in the SCC quantity in the initial feed used during particle formulation up to 30% (w/w); however, the encapsulation efficiency was observed to be the best at a feed ratio of 20% (w/w). *In vitro* efficacy testing of the SCC loaded Ac-DEX nanoparticles demonstrated their activity against both Gram-negative and Gram-positive bacteria; the nanoparticles inhibited the growth of every bacterial species tested. As expected, a higher concentration of drug was required to inhibit bacterial growth when the drug was encapsulated within the nanoparticle formulations compared with the free drug illustrating the desired depot release. Compared with free drug, the Ac-DEX nanoparticles were much more readily suspended in an aqueous phase and subsequently aerosolized, thus providing an effective method of pulmonary drug delivery.

### Keywords

Ac-DEX Particles; Dextran; Silver Carbene Complexes; Antimicrobial; Degradable; Pulmonary Diseases

---

<sup>\*</sup>Corresponding Authors: Professor Jean M. J. Fréchet, Ph.D., 718 Latimer Hall, University of California, Berkeley, Berkeley, CA 94720-1460, USA, Jean.Frechet@kaust.edu.sa, Phone: (510) 643-3077, Fax: (510) 643-3079, Professor Carolyn L. Cannon, M.D., Ph.D., Division of Pulmonary & Vascular Biology, Department of Pediatrics, UT Southwestern Medical Center at Dallas, Dallas, TX 75390-9063, USA, Carolyn.Cannon@UTSouthwestern.edu, Phone: (214) 648-8709, Fax: (214) 648-2096.

<sup>§</sup>Equal contribution first authors.

<sup>\*</sup>Equal contribution corresponding authors.

## Introduction

Infectious diseases constitute the second major cause of death worldwide<sup>1</sup>, and bacteria are the most common source of infection-related death.<sup>2</sup> An increasing number of bacterial infections are evading standard antimicrobial therapies thereby becoming difficult, if not impossible, to treat.<sup>3</sup> Resistance to multiple antibiotics is spreading throughout the world, and the number of reports of therapy failures is growing.<sup>3-6</sup> Traditional antibiotics are no longer effective in all cases, and treatment options for certain microorganisms have become increasingly scarce.<sup>3, 7</sup> Therefore, decreasing the number of deaths caused by bacterial infections will only be possible with the persistent discovery and development of new drugs and drug delivery systems.<sup>5</sup>

In contrast to other antibiotics, silver has been used as an antimicrobial for centuries<sup>8-9</sup>, and yet bacterial resistance to silver is very rare and often transitory. Furthermore, silver has potent antimicrobial efficacy against a broad spectrum of bacteria and has very low toxicity to human cells.<sup>8, 10-11</sup> Consequently, a variety of silver-based compounds have been synthesized and evaluated for their antimicrobial properties.<sup>8-9</sup> For example, silver sulfadiazine was introduced in the 1960s and is still routinely used as an antimicrobial agent in the treatment of burns.<sup>12</sup> Silver nitrate ( $\text{AgNO}_3$ ) has been used as an antimicrobial agent since the 1800s; however, its use is not practical *in vivo* because it interacts with salts and other biological agents present within the bloodstream and rapidly inactivates.<sup>8-9, 13</sup>

Recently, the research groups of Youngs and Cannon have synthesized and evaluated the antimicrobial properties of a series of silver N-heterocyclic carbene complexes (SCCs).<sup>14-17</sup> Excellent reviews on silver and other metal N-heterocyclic carbene complexes detailing their synthesis, properties, and applications are available.<sup>14, 16, 18-19</sup> Even though a few silver carbene complexes (SCC) showed high sensitivity to water and chloride ions<sup>20</sup>, several complexes exhibit improved stability to aqueous solutions and efficient antibacterial activity.<sup>17</sup> However, the *in vivo* efficacy of the SCCs alone may be limited by their rapid clearance, which is typical for small molecule drugs.<sup>21-23</sup> Moreover, silver compounds can react with and be inactivated by sulfur-containing proteins and chloride ions that are present in the bloodstream.<sup>22, 24</sup> Therefore, the development of an appropriate drug delivery system to carry the SCCs should significantly decrease their clearance rate from the body, and could provide protection from external agents present in the bloodstream, increasing the stability and efficacy of the SCCs.

Current research in the drug delivery field is focused on the search and development of new biocompatible and biodegradable materials.<sup>25-27</sup> Micro- or nanoparticles made from degradable polymers, such as polyesters<sup>28</sup>, poly(ortho esters)<sup>29</sup>, and polyanhydrides<sup>30</sup>, have been used as carriers for vaccine applications<sup>31</sup>, gene delivery<sup>32</sup>, and chemotherapeutic agents<sup>33</sup>. Furthermore, several polymers<sup>34</sup>, hyperbranched polymers<sup>35</sup>, and dendrimers<sup>36-37</sup> have been tested as carriers for silver-based antimicrobial compounds.<sup>38-39</sup> Cannon and Wooley *et al.* have successfully encapsulated SCCs into shell crosslinked nanoparticles based on poly(acrylic acid)-*b*-polystyrene (PAA-*b*-PS) copolymers, and established their antimicrobial efficacy *in vitro*, against the Gram-negative pathogens *Escherichia coli* and *Pseudomonas aeruginosa*.<sup>40</sup> Youngs and Cannon *et al.* have loaded SCCs into L-tyrosine polyphosphate nanoparticles (LTP NPs) and demonstrated their activity against several bacterial strains *in vitro* and in a *Pseudomonas aeruginosa* mouse infection model; however, the efficacy of the SCC-LTP NPs seems to be limited by the slow release of the SCC.<sup>41</sup> Thus, our current research interests are focused on the development of biodegradable polymeric nanoparticles for SCCs delivery, in an attempt to improve the efficacy of the drugs through optimizing the loading and release properties of the delivery system.

Dextran, a bacterially derived homopolysaccharide of glucose, is a widely available, FDA-approved biodegradable polymer that demonstrates excellent biocompatibility.<sup>42–43</sup> In addition, dextran already has a history of human use in clinical applications for plasma volume expansion and plasma substitution.<sup>43</sup> Recently, Fréchet has developed a modular and tunable particle system based on acetal-modified dextran (Ac-DEX).<sup>44–45</sup> Masking the hydroxyl groups of dextran as acetals provides a hydrophobic material that is easily processable using various emulsion techniques, while providing tunable pH-sensitivity.<sup>44–45</sup> We have shown that under mildly acidic aqueous conditions (pH= 5.0), the pendant acetal groups hydrolyze, thus unmasking the parent hydroxyl groups of the dextran.<sup>44–45</sup> Ac-DEX particles prepared by emulsion techniques, water in oil (w/o) or water in oil in water (w/o/w) can encapsulate either hydrophobic or hydrophilic molecules, respectively, and the payload release rate can be tuned through the nature of the acetal groups on the dextran.<sup>44–47</sup> The Ac-DEX particles have been successfully tested as vaccine platforms<sup>46, 48</sup> and gene delivery carriers.<sup>49–50</sup> In all cases, payload release was found to occur under mildly acidic conditions, similar to those found in sites of inflammation, tumors, and endocytic vesicles.<sup>44–50</sup>

The present report describes a new method of obtaining biodegradable Ac-DEX nanoparticles of around 100 nm loaded with a hydrophobic silver carbene complex, specifically SCC23. The resulting nanoparticle formulations have been characterized for morphology, size distribution, and silver loading. Subsequently, the activity of the released silver carbene complex from the various formulations has been demonstrated by determination of minimum inhibitory concentration (MIC), minimum bactericidal concentration (MBC), and growth kinetics of various bacterial species in the presence of nanoparticles. Finally, we display the nebulizable characteristics of the SCC loaded Ac-DEX nanoparticle formulations. These results suggest that Ac-DEX nanoparticles encapsulating SCCs may prove to be an effective therapeutic for the treatment of pulmonary bacterial infections.

## Results and discussion

### 1. Synthesis of the Ac-DEX particles

Dextran was reacted with 2-methoxypropene in the presence of an acid catalyst, yielding acetalated-dextran (Ac-DEX). A relatively low reaction time afforded an Ac-DEX polymer, in which most of the acetal groups are acyclic, providing fast degradation rates under mildly acidic conditions.<sup>44–45</sup> For instance, the half-life of the resulting Ac-DEX polymer at pH 5.0 was as short as 15 minutes, which can be significantly increased to 27 hours by employing longer reaction times. The Ac-DEX polymer, unlike the water-soluble dextran polymer, was soluble in organic solvents and completely insoluble in water. This property allowed for the processing of the Ac-DEX polymer into nanoparticles using standard emulsion techniques.<sup>44–46</sup>

For this work, we chose a previously reported polymer with a slow degradation rate<sup>45</sup>, in order to obtain a prolonged antimicrobial effect as a result of a slow release of the antimicrobial agent. As previously described, dextran that has been acetalated for a longer period of time degraded at a slower rate in solution due to a high content of cyclic acetals. In this instance, dextran ( $M_w=10,500$  g/mol) was reacted with 2-methoxypropene in the presence of an acid catalyst for 60 minutes. The extent of coverage of hydroxyl groups, as well as the type of acetals formed, was determined by <sup>1</sup>H-NMR, which demonstrated that 80% of the hydroxyl groups were covered with acetals. The determination of each type of acetal resulted in a degree of substitution (DS, number of hydroxyl modifications per 100 glucose units) of 82 for cyclic acetals and 76 for acyclic acetals.<sup>45</sup> To determine the degradation rate, the particles were suspended in pH 5 or pH 7.4 buffered water at 37 °C. In

pH 5 buffered water, half of the material was degraded after 16h, while there was no significant degradation at neutral pH in the same time frame.

Our previous reports on Ac-DEX particles used an emulsion procedure based on a method reported for the formulation of poly (lactide-co-glycolide) nanocapsules<sup>51</sup>, and usually yielded Ac-DEX particles of around  $250 \pm 100$  nm.<sup>44–46</sup> In the present work, we report a modification of the previous method that was optimized to produce smaller (100 nm) and less polydisperse Ac-DEX particles. The method was optimized by preparing several batches of particles, for which the amount of Ac-DEX polymer (12.5 mg), the amount of organic solvent (0.5 mL), and the sonication conditions were maintained constant. The amount of aqueous solution containing the surfactant (3% PVA in PBS) was varied to achieve several ratios of CH<sub>2</sub>Cl<sub>2</sub>: PBS (1:1, 1:5, 1:10, 1:50), and all data presented here is an average of at least three similar experiments. According to standard emulsion techniques<sup>52–53</sup>, it was expected that varying the ratio of the Ac-DEX organic solution to the aqueous PVA solution would produce nanoparticle populations of different sizes and polydispersities.

For a 1:1 ratio of CH<sub>2</sub>Cl<sub>2</sub>: PBS, the Ac-DEX particles obtained were quite large, with a mean particle size of  $850 \pm 200$  nm (Figure 1, red). By increasing the amount of the aqueous phase, i.e., 1:10 and 1:50 ratios of CH<sub>2</sub>Cl<sub>2</sub>: PBS, the Ac-DEX particles obtained were polydisperse showing a broad peak in the DLS measurement at  $150 \pm 100$  nm and  $200 \pm 100$  nm, respectively. However, when a 1:5 ratio of Ac-DEX CH<sub>2</sub>Cl<sub>2</sub>: PBS was used, the formed Ac-DEX particles presented a relatively low polydispersity with an average size of  $100 \pm 40$  nm (Figure 1). These formulation conditions (1:5 ratio) seemed to be optimal for the formation of Ac-DEX nanoparticles suitable for drug delivery applications. In addition, the SEM characterization of these Ac-DEX particles (Figure 2) showed a particle diameter of  $120 \pm 40$  nm, which is in agreement with the DLS data.

## 2. SCC23 and its loading into Ac-DEX particles

SCC23 (Figure 3) was synthesized from 4,5-dichloroimidazole according to the procedure described in the report by Hindi *et al.*<sup>16</sup> It is hypothesized that the presence of electron withdrawing groups on the 4 and 5 positions of the imidazole ring may lead to a more stable system and this hypothesis was validated through the synthesis and characterization of the dichloroimidazole-based SCCs. The intermediate compound (IC23) was obtained at a 92% yield and characterized using both <sup>1</sup>H NMR and <sup>13</sup>C NMR. The relevant NMR peaks are: <sup>1</sup>H NMR (500 MHz, *d*<sub>6</sub>-DMSO):  $\delta$  5.71 (s, 4H), 7.57–7.62 (m, 6H), 7.95–8.06 (m, 8H), 9.75 (s, 1H) ppm. <sup>13</sup>C NMR (500 MHz, *d*<sub>6</sub>-DMSO):  $\delta$  51.8, 117.9, 119.3, 125.5, 136.7, 136.8, 127.7, 127.8, 128.8, 130.1, 132.7, 132.8, 136.9 ppm. Subsequently, *in situ* deprotonation was carried out with silver acetate to produce the N-heterocyclic carbene silver acetate complex, SCC23, which was obtained at 82.5% yield. Formation of silver carbene complex (SCC23) was confirmed using <sup>1</sup>H NMR, <sup>13</sup>C NMR, elemental analysis, and X-ray analysis and the details are as follows: <sup>1</sup>H NMR (500 MHz, *d*<sub>6</sub>-DMSO):  $\delta$  1.77 (s, 3H), 5.64 (s, 4H), 7.49–7.54 (m, 6H), 7.89–7.94 (m, 8H) ppm. <sup>13</sup>C NMR (500 MHz, *d*<sub>6</sub>-DMSO):  $\delta$  23.5, 28.3, 31.5, 53.7, 63.5, 70.8, 108.6, 140.6, 150.5, 153.0, 175.9, 186.3 ppm. Anal. Calc. for C<sub>27</sub>H<sub>21</sub>AgCl<sub>2</sub>N<sub>2</sub>O<sub>2</sub>: C, 55.51; H, 3.62; N, 4.79%. Found: C, 56.02; H, 3.64; N, 4.77%. Crystal data for SCC23: C<sub>27</sub>H<sub>21</sub>AgCl<sub>2</sub>N<sub>2</sub>O<sub>2</sub>, *M* = 584.23, monoclinic, *a* = 11.905(2) Å, *b* = 19.701(4) Å, *c* = 10.836(2) Å,  $\alpha$  = 90.00°,  $\beta$  = 111.050(3)°,  $\gamma$  = 90.00°, *V* = 2372.0(8) Å<sup>3</sup>, *T* = 100(2) K, space group *P*2(1)/*c*, *Z* = 4,  $\mu$ (MoK $\alpha$ ) = 1.104 mm<sup>-1</sup>, 18642 reflections measured, 4812 independent reflections (*R*<sub>int</sub> = 0.0453). The final *R*<sub>*I*</sub> values were 0.0398 (*I* > 2 $\sigma$ (*I*)). The final *wR*(*F*<sup>2</sup>) values were 0.0944 (*I* > 2 $\sigma$ (*I*)). The final *R*<sub>*I*</sub> values were 0.0549 (all data). The final *wR*(*F*<sup>2</sup>) values were 0.0986 (all data). The goodness of fit on *F*<sup>2</sup> was 1.060.

The presence of aryl functional groups at the 1 and 3 positions on the imidazole ring produced a hydrophobic molecule, which appeared amenable to encapsulation within nanoparticles by a single emulsion procedure. Determination of *in vitro* antimicrobial properties of SCC23 against a panel of clinical bacterial isolates from cystic fibrosis (CF) patients using a standard Clinical and Laboratory Standards Institute (CLSI) protocol demonstrated its excellent activity with an MIC<sub>90</sub> of 2 µg/ml.<sup>54</sup> Furthermore, SCC23 was found to be not only growth-inhibitory, but also bactericidal against all strains of bacteria tested, including the silver resistant bacterial strain *Escherichia coli* J53+pMG101.<sup>54</sup>

Due to the hydrophobicity of SCC23, it was encapsulated into the Ac-DEX particles using a single emulsion procedure similar to that described above, using a 1:5 ratio of CH<sub>2</sub>Cl<sub>2</sub>: PBS. The SCC23 was added to the organic solution together with the Ac-DEX polymer, prior to the emulsion process. Upon particle formation, the SCC23 remained encapsulated in the Ac-DEX particles (Ac-DEX-SCC23). The amount of SCC23 inside the Ac-DEX particles was analyzed by inductively coupled plasma (ICP); the SCC23 loading depended on the initial amount of SCC23 added (Table 1 and Figure 4). The loading of SCC23 increased significantly up to 30% initial feed, reaching 154 µg of SCC23 *per* mg of particle (for Ac-DEX-SCC23-3, Table 1). However, for higher initial feeds the final loading of SCC23 was not significantly higher. The highest loading efficiency was achieved using an initial feed of 20% (w/w) of SCC23, resulting in a 13% (w/w) loading of the SCC.

The size of the Ac-DEX-SCC23 particles was analyzed immediately following the sonication process, and at that point, all batches of particles measured between 100–150 nm. After centrifugation, washing with water, lyophilization, and re-dispersion in PBS, the size of the particles was measured again. At this time point, the particles with an initial SCC23 feed of higher than 30% demonstrated a strong tendency to aggregate; Ac-DEX-SCC23-4 and Ac-DEX-SCC23-5 measured around 700 nm (Figures S4 and S5, Sup. Inf.). When the Ac-DEX-NPs were formed in the presence of such large amounts of hydrophobic SCC (40 and 50% w/w), a significant amount of the SCC likely remained outside of the NP, such that after lyophilization, the external hydrophobic SCC prevented the redispersion of NPs. Due to the aggregation tendency, no further experiments were performed with these two batches of particles. Ac-DEX-SCC23-1, Ac-DEX-SCC23-2, and Ac-DEX-SCC23-3 nanoparticle formulations did not show a tendency to aggregate, and no significant difference in their sizes after the lyophilization process was observed. Particles in each of these three formulations remained in the 100–120 nm size range (Table 1 and Figure S1–S3 of Sup. Inf.).

In addition, the Ac-DEX-SCC23 particles were characterized by TEM in order to confirm their size range and the presence of silver inside the particles. The size of Ac-DEX-SCC23 particles found by TEM was slightly smaller than the size obtained by DLS: a) empty Ac-DEX particles, size by TEM: 140 ± 40 nm; b) Ac-DEX-SCC23-1 particles loaded with 6.0 % w/w SCC23, size by TEM: 80 ± 40 nm; c) Ac-DEX-SCC23-2 particles loaded with 13.0 % w/w SCC23, size by TEM: 100 ± 40 nm; d) Ac-DEX-SCC23-3 particles loaded with 15.4 % w/w SCC23, size by TEM: 90 ± 40 nm (Figure 5). The larger particle sizes observed by DLS compared with TEM measurements are due to differences in the state of the particles during the measurements; the diameter data obtained by DLS includes the outer solvent layer that surrounds the nanoparticles, whereas the TEM measurements are performed when the particles are in a dry state.

### 3. Antibacterial activity of the Ac-DEX-SCC23 nanoparticles

The antibacterial activity of the Ac-DEX-SCC23 nanoparticle formulations was tested against both Gram-negative and Gram-positive bacteria. The minimum inhibitory concentration (MIC), minimum bactericidal concentration (MBC), and the growth kinetics

of the bacteria were investigated in the presence of various nanoparticle formulations and compared with those of the free SCC23 drug. Again, SCC23 has been shown to be highly active against all tested microorganisms; its MIC<sub>90</sub> was found to be 2 µg/ml for non-silver resistant organisms tested<sup>54</sup> Furthermore, while other SCCs to date have not demonstrated considerable activity against the silver resistant *E. coli* J53 + pMG101 strain (MIC > 20 µg/ml), the MIC of SCC23 against the same *E. coli* species was found to be 6 µg/ml.<sup>54</sup> Additionally, SCC23 was found to be bactericidal against all strains of bacteria tested.<sup>54</sup>

Determination of MIC and MBC of various nanoparticle formulations against representative Gram-negative and Gram-positive bacteria demonstrated that the SCC23 released from the Ac-DEX-SCC23 nanoparticles remained active in all cases. The SCC23 concentrations, at which inhibitory and bactericidal effects were observed, were the highest for the silver resistant strain *E. coli* J53 + pMG101 and the lowest for the silver sensitive strain *E. coli* J53. These results are in agreement with our previous observations with free SCC23.<sup>54</sup> Ac-DEX-SCC23 nanoparticle formulations were also inhibitory and bactericidal to two strains of *Pseudomonas aeruginosa*, as well as a methicillin-resistant strain of *Staphylococcus aureus* as demonstrated in Table 2. Interestingly, for most of the bacteria, not all of the formulations were effective in inhibiting bacterial growth or killing bacteria at the same theoretical concentration of SCC23. The different outcomes observed for the various Ac-DEX-SCC23 formulations, despite the constant theoretical concentration of SCC23 constant in each case, likely resulted from differences in the release rate of SCC23 from the Ac-DEX nanoparticles coupled with differences in the activity of SCC23 against the various bacterial species. Furthermore, encapsulating SCC23 within Ac-DEX nanoparticles resulted in an increase in the apparent MIC of the SCC23 component, as one would expect due to the slow release and hence, lower free Ag (I) concentration at any given SCC23 concentration. Empty Ac-DEX nanoparticles had no antimicrobial activity in these assays.

An investigation into the growth kinetics of bacteria following exposure to various Ac-DEX-SCC23 nanoparticle formulations further demonstrated the ability of the nanoparticles to inhibit bacterial growth (Table 3, Figures 6–9). As expected, growth was observed when each of the bacteria was exposed to either control solution or empty Ac-DEX nanoparticles only. Furthermore, at the lowest SCC23 concentration of 0.4 µg/well, bacterial growth was observed in all cases (Table 3). When *Pseudomonas aeruginosa* strain PA 01 (Figure 6) and methicillin-resistant *Staphylococcus aureus* strain SA LL06 (Figure 8) were exposed to 0.4 microgram of SCC23, growth was observed for each of the Ac-DEX-SCC23 formulations; however, the lag periods prior to bacterial growth were found to be significantly different. For instance, following PA 01 exposure to 0.4 microgram SCC23 (Ac-DEX-SCC23-1), bacterial growth began at approximately 2 hours; whereas, the bacterial growth started at approximately 5 (Ac-DEX-SCC23-3) and 8 hours (Ac-DEX-SCC23-2), respectively following exposure to 0.4 microgram SCC23. Finally, when *E. coli* J53 bacteria were exposed to various formulations of Ac-DEX-SCC23 nanoparticles (Figure 9), no growth of the bacteria was observed at SCC23 concentrations of 1.6 microgram and higher. However, the growth inhibition of the same bacteria incorporating the silver resistant plasmid pMG101 (*E. coli* J53 + pMG101) was observed at a higher SCC23 concentration of 3.2 microgram. These results are similar to the outcome observed when MIC/MBC experiments were performed with *E. coli* J53 + pMG101 using the SCC23 loaded Ac-DEX nanoparticles (Table 2). Our previous results demonstrate an MIC of 6 µg/ml for the *E. coli* J53 + pMG101 bacteria using free SCC23 (unencapsulated form).<sup>54</sup> The difference in concentration at which growth inhibition was observed between the free drug and the nanoparticle formulations possibly resulted from the manner in which the bacteria were exposed to silver. In the case of the free drug, the bacteria were exposed to silver instantaneously; in case of nanoparticles, a constant antibiotic pressure is maintained on the bacteria due to the depot delivery afforded by the nanoparticles. The ability of SCC23 to

inhibit the growth of bacteria harboring a silver resistance plasmid suggested that the carbene carrier molecule may be enhancing the antimicrobial efficacy of the final SCC compound. Once the carbene carrier is degraded or metabolized in case of the free drug treatment, the bacteria may be able to overcome the inhibitory effects of the SCC and demonstrate growth, thus exhibiting a higher MIC value.

#### 4. Evaluation of the nebulization efficacy of the Ac-DEX-SCC23 nanoparticles

The efficiency of nebulization using micropump technology has appeared to be a function of the ionic strength of the liquid, i.e., solutions with higher ionic strength nebulize more readily.<sup>55</sup> Therefore, different solutions may be nebulized with different efficiencies, as has been found by us and by several other researchers.<sup>55</sup> Generally, Ac-DEX particles have demonstrated a negative zeta-potential, that is, an anionic surface, which would facilitate nebulization. To further ensure efficient nebulization of the nanoparticles, they were suspended in phosphate buffer. An aliquot of the resulting suspension was placed into the Aeroneb Lab nebulizer and the aerosolized suspension was collected and analyzed using optical microscopy. As expected, the nebulization of phosphate buffer alone was free of nanoparticles; whereas, the condensate from the nebulized Ac-DEX nanoparticles showed a plethora of nanoparticles demonstrating that NPs readily passed through the nebulizer (Figure 10). These results suggested that nebulization of Ac-DEX NPs was a viable method for localized delivery of antimicrobials to the lungs.

### Conclusion

Ac-DEX nanoparticles encapsulating a hydrophobic silver carbene complex antimicrobial were prepared by a single-emulsion process. By controlling the ratio of the organic phase to the aqueous phase while keeping other parameters, such as polymer quantity and sonication conditions constant, discrete, smooth, and spherical nanoparticles with an average diameter of  $100 \pm 40$  nm and a low polydispersity were prepared. These results were further confirmed by DLS, SEM, and TEM characterization. Silver loading within the Ac-DEX nanoparticles was found to increase with an increase in the initial feed up to 30% and the encapsulation efficiency was observed to be between 51 – 65% suggesting that a high therapeutic payload could be achieved within the nanoparticles. Furthermore, a comparison of the average particle size pre- and post-lyophilization demonstrates no changes in the particle size due to the lyophilization process, confirming the stability of the particles. MIC/MBC studies and determination of bacterial growth kinetics demonstrated that Ac-DEX-SCC23 nanoparticle formulations were bactericidal against all bacterial strains tested including the silver-resistant strain, *E. coli J53+pMG101*. The observed differences in the antimicrobial activity among different nanoparticle formulations at the same theoretical SCC23 dose, however, suggested that the efficacy of the nanoparticles is a function of the release kinetics of silver from the particles. Finally, the Ac-DEX nanoparticles were found to readily nebulize in a phosphate buffer medium, thus providing a simple and efficacious method for localized pulmonary delivery of hydrophobic antimicrobials.

### Experimental section

#### General considerations

The Ac-DEX polymer was synthesized in one step from dextran, according to our previous report.<sup>45</sup> The SCC23 was synthesized in a multi-step process from 4, 5-dichloroimidazole as described by Hindi *et al.*<sup>16</sup> Reagents for SCC23 synthesis were purchased from Alfa Aesar, solvents from Fisher Scientific, and all were used without further purification. Reactions proceeded under aerobic conditions. <sup>1</sup>H and <sup>13</sup>C NMR data were obtained with a Varian 500 MHz instrument and spectra were referenced to deuterated solvents. Elemental analyses

were performed by the University of Illinois microanalysis laboratory. Crystal structure data sets were collected using a Bruker SMART Apex CCD diffractometer with graphite-monochromated Mo K $\alpha$  radiation ( $\lambda = 0.71073 \text{ \AA}$ ). Unit cell determination was achieved by collecting reflections from three different orientations.

### Synthesis of IC23

4,5-dichloroimidazole (10.0 mmol, 1.370 g) and KOH (11.0 mmol, 0.617 g) were placed in a 50 mL round bottom flask with 10 mL acetonitrile. The mixture was brought to reflux (85°C) and stirred 1h until KOH was consumed. Bromomethylnaphthalene (10.00 mmol, 2.211 g) was added and the solution was stirred 2.5 hours. KBr was removed by vacuum filtration and a second equivalent of bromomethylnaphthalene was added to the filtrate. The mixture was stirred at reflux for 1.5 hours. The white precipitate was collected by filtration and analyzed (IC23).

### Synthesis of SCC23

Compound IC23 (5.00 mmol, 2.491 g) was dissolved in chloroform in a 50 mL round bottom flask. Silver acetate (10.00 mmol, 1.669 g) was added and the mixture was stirred at room temperature 2 hours. A solid precipitate, presumably silver bromide, was removed by vacuum filtration through celite and the volatiles were removed from the filtrate by rotary evaporation. Ethyl ether was added to precipitate SCC23, which was collected by filtration and dried under vacuum.

### Dynamic Light-Scattering measurements (DLS)

Particle size distributions and average particle diameters were determined by dynamic light scattering using a Zetasizer Nano ZS (Malvern Instruments, United Kingdom). Particles were suspended in PBS (pH 7.4) and three measurements were taken of the resulting dispersions.

### Inductively coupled plasma (ICP)

The silver content in the Ac-DEX nanoparticles was analyzed in a Perkin Elmer precisely optical emission spectrometer, Optima 7000DV. The nanoparticles were dissolved in a 5% HNO<sub>3</sub> aqueous solution prior to analysis. Prior to every measurement, the instrument was calibrated with solutions of a commercial silver standard for ICP (0.1 mg/L, 1.0 mg/L, 5.0 mg/L, 10 mg/L, 50 mg/L).

### Scanning Electron Microscopy (SEM)

The Ac-DEX nanoparticles were suspended in PBS and dripped onto silicon wafers. The samples were dried overnight under a hood, and sputter coated with a 2 nm layer of a palladium/gold alloy. The images were obtained using the scanning electron microscope S-5000 microscope (Hitachi).

### Transmission Electron Microscopy (TEM)

Ac-DEX nanoparticles were characterized by transmission electron microscopy with a FEI Tecnai 12 Transmission electron microscope. The sample solutions were deposited onto a carbon-coated copper grid, and after 3 minutes excess solvent was removed.

### Preparation of the empty Ac-DEX nanoparticles by single mini-emulsion

Ac-DEX nanoparticles were prepared by using a single-emulsion oil/water (o/w) method. Ac-DEX (100 mg) was dissolved in CH<sub>2</sub>Cl<sub>2</sub> (4.0 mL). An aqueous solution of poly(vinyl alcohol) (PVA,  $M_w$ : 13,000–23,000 g/mol, 87–89% hydrolyzed) (20 mL, 3% wt/wt in PBS)



was added and the mixture was sonicated for 30s on ice by using a probe sonicator (Branson Sonifier 450) with an output setting of 5 and a duty cycle of 70%. The size of the particles was measured by DLS just after sonication. The solutions were then stirred for about 3h, allowing the organic solvent to evaporate. The particles were isolated by centrifugation (25,000 rpm, 30 min), and washed with dd-H<sub>2</sub>O (pH adjusted to 8.0) by redispersing, centrifuging and removal of supernatant. The washed particles were lyophilized to yield white powders. After lyophilization, the particles were easily redispersed in PBS by vortexing and bath sonicating (VWR Ultrasonic Cleaner 750) for a few minutes, and their size was measured again by DLS.

### Preparation of the Ac-DEX-SCC23 nanoparticles by single mini-emulsion

The Ac-DEX particles containing SCC23 were prepared following a similar procedure than the one described for the empty Ac-DEX particles, in which the SCC23 was added to the CH<sub>2</sub>Cl<sub>2</sub> solution of Ac-DEX polymer prior to addition of the aqueous solution.

### Bacteria

The laboratory strain PAO1-V was provided by Dr. Maynard Olson (University of Washington, Seattle). The mucoid clinical isolate of *P. aeruginosa* PA M57-15 was provided by Dr. Thomas Ferkol (Washington University, St. Louis, MO). The SA LL06 strain was cultured from the sputum of cystic fibrosis patients at St. Louis Children's Hospital. The silver sensitive and silver resistant *E. coli* strains J53 and J53+pMG101, were provided by Dr. Simon Silver (University of Chicago, Chicago, IL). The J53 strain is known to be sensitive to killing by silver cations and serves as a positive control. In contrast, the J53+pMG101 is a J53 derivative that harbors the pMG101 plasmid originally conferring silver resistance to a burn ward isolate of *Salmonella* and serves as a negative control. All bacterial strains were maintained as glycerol stocks at -80 °C.

### MIC-MBC determination and bacterial growth assay

Minimal inhibitory concentrations (MICs) were determined by broth microdilution method as previously described by a standard Clinical and Laboratory Standards Institute (CLSI) protocol. Briefly, bacteria were streaked from frozen glycerol stocks onto TSA plates and incubated overnight at 37 °C. Colonies from the fresh plates were suspended in the CLSI standard M-H broth to an optical density at 650 nm (OD<sub>650</sub>) of 0.2 and grown at 37 °C in a shaking incubator at 200 rpm to an OD<sub>650</sub> of 0.4, which corresponds to ~5 x 10<sup>8</sup> colony forming units (CFU)/mL. The bacteria were diluted in the broth to a concentration of 10<sup>5</sup> in 100 µL, which was added to triplicate wells of a 96-well plate. Three different formulations of Ac-DEX NPs encapsulating SCC23 were resuspended in sterile distilled-deionized water (DH<sub>2</sub>O) to achieve a maximum SCC23 concentration of 128 µg/ml. The nanoparticles were thoroughly re-suspended by sonication for 1 minute at 70% amplitude (SONICS® Vibra-cell VCX130, Sonics & Materials, Inc., Newtown, CT). Two-fold serial dilutions of the nanoparticle suspensions were performed to achieve SCC concentrations of 128, 64, 32, 16, and 8 µg/ml. 100 µL of the nanoparticle suspensions at various SCC concentrations were also added to triplicate wells of a 96-well plate containing the bacteria to achieve a final SCC concentration of 6.4, 3.2, 1.6, 0.8, and 0.4 µg/well. Blank nanoparticles suspended in DH<sub>2</sub>O, M-H broth, free SCC23 and tobramycin were used as controls. SCC23 (in DMSO) and tobramycin (in DH<sub>2</sub>O) solutions were prepared as stock solutions at 10 mg/mL and diluted in DH<sub>2</sub>O to appropriate concentrations. The plates were incubated overnight at 37 °C. The MIC was the lowest of these concentrations, at which each of the triplicate wells in each 96-well plate was clear after 16–24 h incubation. Each triplicate measurement was performed at least in duplicate for a minimum of 6 separate measurements. The MBC of various SCC compounds was determined by plating the wells with growth inhibition (clear)

on TSA plates and noting the lowest concentration that resulted in no growth after an overnight incubation at 37 °C.

To perform bacterial growth assay, the above-mentioned bacteria were streaked from glycerol-frozen stocks onto TSA plates and incubated overnight at 37°C. Cells were grown as described above and 100 µL of the bacterial suspension at OD<sub>650</sub> of 0.4 was added to the wells of a 96-well plate. Serial dilutions of the three formulations of SCC23-Ac-DEX NPs were performed as described previously and added to the wells of a 96-well plate in triplicate containing the bacteria. Blank nanoparticles suspended in DH<sub>2</sub>O and M-H broth with and without 5% DMSO were used as controls. The 96-well plate was placed in a shaking microplate reader (BioTek Synergy HT, BioTek Instruments, Inc., Winooski, VT) overnight at 37°C with OD<sub>650</sub> readings every 10 minutes. Data were graphed using Prism 5 (GraphPad Software, Inc., San Diego, CA).

### Nebulization potential of Ac-DEX nanoparticles

Formulations of Ac-DEX nanoparticles loaded with SCC23 were reconstituted in 5 ml of phosphate buffer (18 mg/ml Na<sub>2</sub>HPO<sub>4</sub> and 3 mg/ml KH<sub>2</sub>PO<sub>4</sub>) to a concentration of 5 mg/ml, respectively. The solution contained no Cl<sup>-</sup> ions to avoid precipitation of AgCl. The reconstituted Ac-DEX NPs and phosphate buffer (control) were delivered via an Aeroneb Lab apparatus (Aerogen Inc., Galway, Ireland) connected to a multi-dosing animal chamber. The Aerogen nebulizer is based on micropump technology that produces fine particles (1–5 µm) in a low velocity aerosol.<sup>56</sup> The multi-dosing chamber is a square Plexiglas box with inner dimensions of 8 x 8 x 4.5 inches height. The nebulizer is mounted in the center of the lid. To test whether the Ac-DEX NPs could be easily nebulized, the nanoparticle suspensions prepared as described above were placed into the nebulizer, aerosolized, and the vapor was collected directly into a 50 ml conical tube. The condensed mist was placed on a glass slide and examined under a Zeiss Axioplan microscope. Microscopy images were acquired using Axiovision software.

### Supplementary Material

Refer to Web version on PubMed Central for supplementary material.

### Acknowledgments

This project has been funded in part with Federal funds from the National Heart, Lung, and Blood Institute, National Institutes of Health, Department of Health and Human Services, under Contract No. HHSN268201000043C, and in part through the Fréchet “various gifts” fund for the support of research in new materials. Dr. Peter R. Wich gratefully acknowledges the Alexander von Humboldt Foundation (AvH) for funding.

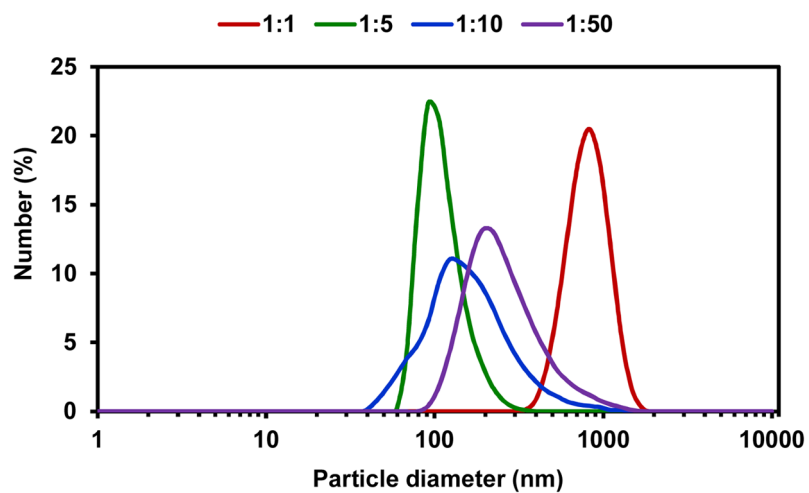
### References

1. World Health Report. World Health Organization; Geneva: 2011.
2. Jones KE, Patel NG, Levy MA, Storeygard A, Balk D, Gittleman JL, Daszak P. Global trends in emerging infectious diseases. *Nature*. 2008; 451(7181):990–3. [PubMed: 18288193]
3. von Nussbaum F, Brands M, Hinzen B, Weigand S, Habich D. Antibacterial natural products in medicinal chemistry--exodus or revival? *Angew Chem Int Ed Engl*. 2006; 45(31):5072–129. [PubMed: 16881035]
4. Walsh FM, Amyes SG. Microbiology and drug resistance mechanisms of fully resistant pathogens. *Curr Opin Microbiol*. 2004; 7(5):439–44. [PubMed: 15451497]
5. Coates AR, Halls G, Hu Y. Novel classes of antibiotics or more of the same? *Br J Pharmacol*. 2011; 163(1):184–94. [PubMed: 21323894]
6. Simoes M. Antimicrobial strategies effective against infectious bacterial biofilms. *Curr Med Chem*. 2011; 18(14):2129–45. [PubMed: 21517762]

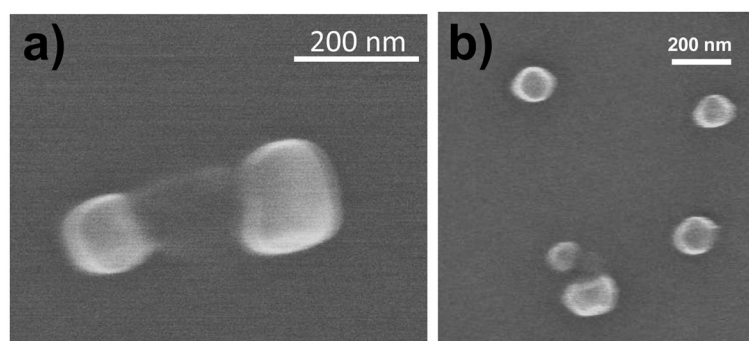
7. Wenzel RP, Edmond MB. Managing antibiotic resistance. *N Engl J Med.* 2000; 343(26):1961–3. [PubMed: 11136269]
8. Russell, AD.; Hugo, WB. Antimicrobial Activity and Action of Silver. In: Ellis, GP.; Luscombe, DK., editors. *Progress in Medicinal Chemistry.* Vol. 31. Elsevier; Amsterdam: 1994. p. 351-370.
9. Knetsch MLW, Koole LH. New strategies in the development of antimicrobial coatings: The example of increase usage of silver and silver nanoparticles. *Polymers.* 2011; 3(1):340–366.
10. Silver S. Bacterial silver resistance: molecular biology and uses and misuses of silver compounds. *FEMS Microbiol Rev.* 2003; 27(2–3):341–53. [PubMed: 12829274]
11. Percival SL, Bowler PG, Russell D. Bacterial resistance to silver in wound care. *J Hosp Infect.* 2005; 60(1):1–7. [PubMed: 15823649]
12. Fox CL Jr. Silver sulfadiazine--a new topical therapy for *Pseudomonas* in burns. Therapy of *Pseudomonas* infection in burns. *Arch Surg.* 1968; 96(2):184–8. [PubMed: 5638080]
13. Moyer CA. Some effects of 0.5 per cent silver nitrate and high humidity upon the illness associated with large burns. *J Natl Med Assoc.* 1965; 57(2):95–100. [PubMed: 5863945]
14. Garrison JC, Youngs WJ. Ag(I) N-heterocyclic carbene complexes: synthesis, structure, and application. *Chem Rev.* 2005; 105(11):3978–4008. [PubMed: 16277368]
15. Kascatan-Nebioglu A, Melaiye A, Hindi K, Durmus S, Panzner MJ, Hogue LA, Mallett RJ, Hovis CE, Coughenour M, Crosby SD, Milsted A, Ely DL, Tessier CA, Cannon CL, Youngs WJ. Synthesis from caffeine of a mixed N-heterocyclic carbene-silver acetate complex active against resistant respiratory pathogens. *J Med Chem.* 2006; 49(23):6811–8. [PubMed: 17154511]
16. Hindi KM, Panzner MJ, Tessier CA, Cannon CL, Youngs WJ. The medicinal applications of imidazolium carbene-metal complexes. *Chem Rev.* 2009; 109(8):3859–84. [PubMed: 19580262]
17. Panzner MJ, Deeraksa A, Smith A, Wright BD, Hindi KM, Kascatan-Nebioglu A, Torres AG, Judy BM, Hovis CE, Hilliard JK, Mallett RJ, Cope E, Estes DM, Cannon CL, Leid JG, Youngs WJ. Synthesis and in vitro Efficacy Studies of Silver Carbene Complexes on Biosafety Level 3 Bacteria. *Eur J Inorg Chem.* 2009; 2009(13):1739–1745. [PubMed: 20160993]
18. Lin IJB, Vasam CS. Preparation and application of N-heterocyclic carbene complexes of Ag(I). *Coord Chem Rev.* 2007; 251:642–670.
19. Lin JCY, Huang RTW, Lee CS, Bhattacharyya A, Hwang WS, Lin IJB. Coinage Metal - N-heterocyclic carbene complexes. *Chem Rev.* 2009; 109:3561–3598. [PubMed: 19361198]
20. Hindi KM, Siciliano TJ, Durmus S, Panzner MJ, Medvetz DA, Reddy DV, Hogue LA, Hovis CE, Hilliard JK, Mallett RJ, Tessier CA, Cannon CL, Youngs WJ. Synthesis, stability, and antimicrobial studies of electronically tuned silver acetate N-heterocyclic carbenes. *J Med Chem.* 2008; 51(6):1577–83. [PubMed: 18288795]
21. Owusu-Ababio G, Rogers J, Anwar H. Effectiveness of ciprofloxacin microspheres in eradicating bacterial biofilm. *J Control Release.* 1999; 57(2):151–9. [PubMed: 9971894]
22. Patton JS, Fishburn CS, Weers JG. The lungs as a portal of entry for systemic drug delivery. *Proc Am Thorac Soc.* 2004; 1(4):338–44. [PubMed: 16113455]
23. Fox ME, Szoka FC, Frechet JM. Soluble polymer carriers for the treatment of cancer: the importance of molecular architecture. *Acc Chem Res.* 2009; 42(8):1141–51. [PubMed: 19555070]
24. Meers P, Neville M, Malinin V, Scotto AW, Sardaryan G, Kurumunda R, Mackinson C, James G, Fisher S, Perkins WR. Biofilm penetration, triggered release and in vivo activity of inhaled liposomal amikacin in chronic *Pseudomonas aeruginosa* lung infections. *J Antimicrob Chemother.* 2008; 61(4):859–68. [PubMed: 18305202]
25. Green, JJ.; Zugates, GT.; Langer, R.; Anderson, DG. Poly ( $\beta$ -amino esters): Procedures for Synthesis and Gene Delivery. In: Belting, M., editor. *Macromolecular Drug Delivery.* Vol. 480. Humana Press; 2009. p. 53-63.
26. Ulery BD, Nair LS, Laurencin CT. Biomedical Applications of Biodegradable Polymers. *J Polym Sci B Polym Phys.* 2011; 49(12):832–864. [PubMed: 21769165]
27. Tran VT, Benoit JP, Venier-Julienne MC. Why and how to prepare biodegradable, monodispersed, polymeric microparticles in the field of pharmacy? *International Journal of Pharmaceutics.* 2011; 407:1–11.
28. Yolles S, Leafé TD, Meyer FJ. Timed-release depot for anticancer agents. *J Pharm Sci.* 1975; 64(1):115–6. [PubMed: 166155]

29. Heller J, Barr J, Ng SY, Shen HR, Schwach-Abdellaoui K, Einmahl S, Rothen-Weinhold A, Gurny R. Poly(ortho esters) - their development and some recent applications. *Eur J Pharm Biopharm.* 2000; 50(1):121–8. [PubMed: 10840196]
30. Rosen HB, Chang J, Wnek GE, Linhardt RJ, Langer R. Bioerodible polyanhydrides for controlled drug delivery. *Biomaterials.* 1983; 4(2):131–3. [PubMed: 6860755]
31. Solbrig CM, Saucier-Sawyer JK, Cody V, Saltzman WM, Hanlon DJ. Polymer nanoparticles for immunotherapy from encapsulated tumor-associated antigens and whole tumor cells. *Mol Pharm.* 2007; 4(1):47–57. [PubMed: 17217312]
32. Koby G, Ofra B, Dganit D, Marcelle M. Poly (D, L-lactide-co-glycolide acid) nanoparticles for DNA delivery: Waiving preparation complexity and increasing efficiency. *Biopolymers.* 2007; 85:379–391. [PubMed: 17266128]
33. Sengupta S, Eavarone D, Capila I, Zhao G, Watson N, Kiziltepe T, Sasisekharan R. Temporal targeting of tumour cells and neovasculature with a nanoscale delivery system. *Nature.* 2005; 436(7050):568–72. [PubMed: 16049491]
34. Sambhy V, MacBride MM, Peterson BR, Sen A. Silver bromide nanoparticle/polymer composites: dual action tunable antimicrobial materials. *J Am Chem Soc.* 2006; 128(30):9798– 808. [PubMed: 16866536]
35. Aymonier C, Schlotterbeck U, Antonietti L, Zacharias P, Thomann R, Tiller JC, Mecking S. Hybrids of silver nanoparticles with amphiphilic hyperbranched macromolecules exhibiting antimicrobial properties. *Chem Commun (Camb).* 2002; (24):3018–9. [PubMed: 12536795]
36. Balogh L, Swanson DR, Tomalia DA, Hagnauer GL, McManus AT. Dendrimer- silver complexes and nanocomposites as antimicrobial agents. *Nano Letters.* 2001; 1(1):18–21.
37. Astruc D, Boisselier E, Ornelas C. Dendrimers designed for functions: from physical, photophysical, and supramolecular properties to applications in sensing, catalysis, molecular electronics, photonics, and nanomedicine. *Chem Rev.* 2010; 110(4):1857–959. [PubMed: 20356105]
38. Marambio-Jones C, Hoek EM. A review of the antibacterial effects of silver nanomaterials and potential implications for human health and the environment. *Journal of Nanoparticle Research.* 2010; 12(5):1531–1551.
39. Dallas P, Sharma VK, Zboril R. Silver polymeric nanocomposites as advanced antimicrobial agents: classification, synthetic paths, applications, and perspectives. *Adv Colloid Interface Sci.* 2011; 166(1–2):119–35. [PubMed: 21683320]
40. Li Y, Hindi K, Watts KM, Taylor JB, Zhang K, Li Z, Hunstad DA, Cannon CL, Youngs WJ, Wooley KL. Shell crosslinked nanoparticles carrying silver antimicrobials as therapeutics. *Chem Commun (Camb).* 2010; 46(1):121–3. [PubMed: 20024313]
41. Hindi KM, Ditto AJ, Panzner MJ, Medvetz DA, Han DS, Hovis CE, Hilliard JK, Taylor JB, Yun YH, Cannon CL, Youngs WJ. The antimicrobial efficacy of sustained release silver-carbene complex-loaded L-tyrosine polyphosphate nanoparticles: characterization, in vitro and in vivo studies. *Biomaterials.* 2009; 30(22):3771–9. [PubMed: 19395021]
42. Hermanson, GT. *Bioconjugate Techniques.* Academic Press; San Diego: 1996.
43. Naessens M, Cerdobbel A, Soetaert W, Vandamme EJ. *Leuconostoc* dextranucrase and dextran: production, properties, and applications. *Journal of Chemical Technology and Biotechnology.* 2005; 80(8):845–860.
44. Bachelder EM, Beaudette TT, Broaders KE, Dashe J, Frechet JM. Acetal-derivatized dextran: an acid-responsive biodegradable material for therapeutic applications. *J Am Chem Soc.* 2008; 130(32):10494–5. [PubMed: 18630909]
45. Broaders KE, Cohen JA, Beaudette TT, Bachelder EM, Frechet JM. Acetalated dextran is a chemically and biologically tunable material for particulate immunotherapy. *Proc Natl Acad Sci U S A.* 2009; 106(14):5497–502. [PubMed: 19321415]
46. Bachelder EM, Beaudette TT, Broaders KE, Frechet JM, Albrecht MT, Mateczun AJ, Ainslie KM, Pesce JT, Keane-Myers AM. In vitro analysis of acetalated dextran microparticles as a potent delivery platform for vaccine adjuvants. *Mol Pharm.* 2010; 7(3):826– 35. [PubMed: 20230025]

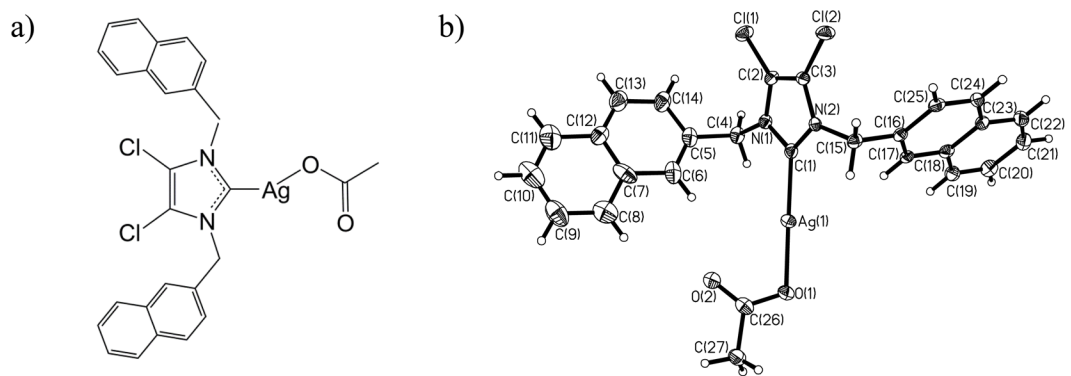
47. Beaudette TT, Cohen JA, Bachelder EM, Broaders KE, Cohen JL, Engleman EG, Frechet JM. Chemoselective ligation in the functionalization of polysaccharide-based particles. *J Am Chem Soc.* 2009; 131(30):10360–1. [PubMed: 19591467]
48. Cui L, Cohen JA, Broaders KE, Beaudette TT, Frechet JM. Mannosylated dextran nanoparticles: a pH-sensitive system engineered for immunomodulation through mannose targeting. *Bioconjug Chem.* 2011; 22(5):949–57. [PubMed: 21476603]
49. Cohen JA, Beaudette TT, Cohen JL, Broaders KE, Bachelder EM, Frechet JM. Acetal-modified dextran microparticles with controlled degradation kinetics and surface functionality for gene delivery in phagocytic and non-phagocytic cells. *Adv Mater.* 2010; 22(32):3593–7. [PubMed: 20518040]
50. Cohen JL, Schubert S, Wich PR, Cui L, Cohen JA, Mynar JL, Frechet JM. Acid- degradable cationic dextran particles for the delivery of siRNA therapeutics. *Bioconjug Chem.* 2011; 22(6): 1056–65. [PubMed: 21539393]
51. Bilati U, Allemann E, Doelker E. Sonication parameters for the preparation of biodegradable nanocapsules of controlled size by the double emulsion method. *Pharm Dev Technol.* 2003; 8(1): 1–9. [PubMed: 12665192]
52. Anton N, Vandamme TF. Nano-emulsions and micro-emulsions: clarifications of the critical differences. *Pharm Res.* 2011; 28(5):978–85. [PubMed: 21057856]
53. Landfester, K.; Musyanovych, A. Hydrogels in Miniemulsions. In: Pich, A.; Richtering, W., editors. *Chemical Design of Responsive Microgels.* Vol. 234. Springer; Heidelberg: 2011. p. 39-63.
54. Leid JG, Ditto AJ, Knapp A, Shah PN, Wright BD, Blust R, Christensen L, Clemons CB, Wilber JP, Young GW, Kang AG, Panzner MJ, Cannon CL, Yun YH, Youngs WJ, Seckinger NM, Cope EK. In vitro antimicrobial studies of silver carbene complexes: activity of free and nanoparticle carbene formulations against clinical isolates of pathogenic bacteria. *J Antimicrob Chemother.* 2011
55. Zhang G, David A, Wiedmann TS. Performance of the vibrating membrane aerosol generation device: Aeroneb Micropump Nebulizer. *J Aerosol Med.* 2007; 20(4):408–16. [PubMed: 18158713]
56. Geller DE, Rosenfeld M, Waltz DA, Wilmott RW. Efficiency of pulmonary administration of tobramycin solution for inhalation in cystic fibrosis using an improved drug delivery system. *Chest.* 2003; 123(1):28–36. [PubMed: 12527599]



**Figure 1.** DLS data obtained for the particles prepared by different formulation procedures. Particle size distribution as a function of various ratios of CH<sub>2</sub>Cl<sub>2</sub>: PBS (1:1, 1:5, 1:10, 1:50) are depicted.

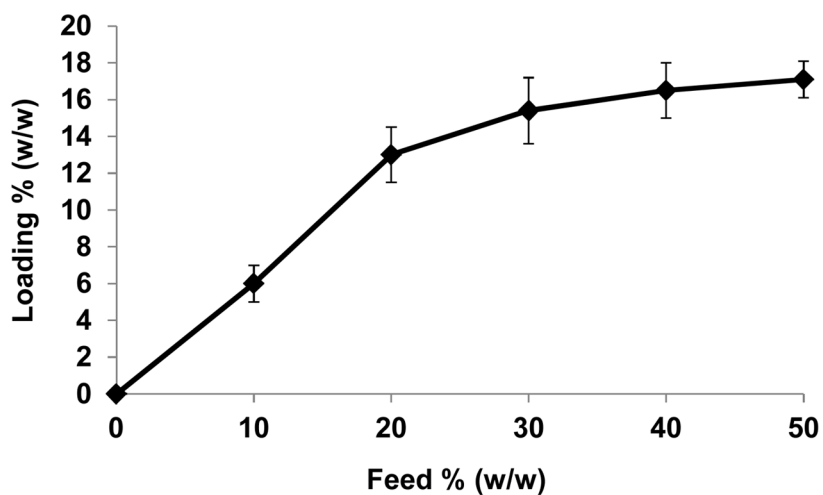


**Figure 2.**  
SEM images of empty Ac-DEX particles prepared using a 1:5 ratio of Ac-DEX  
 $\text{CH}_2\text{Cl}_2$ :PBS ( $120 \pm 40$  nm).

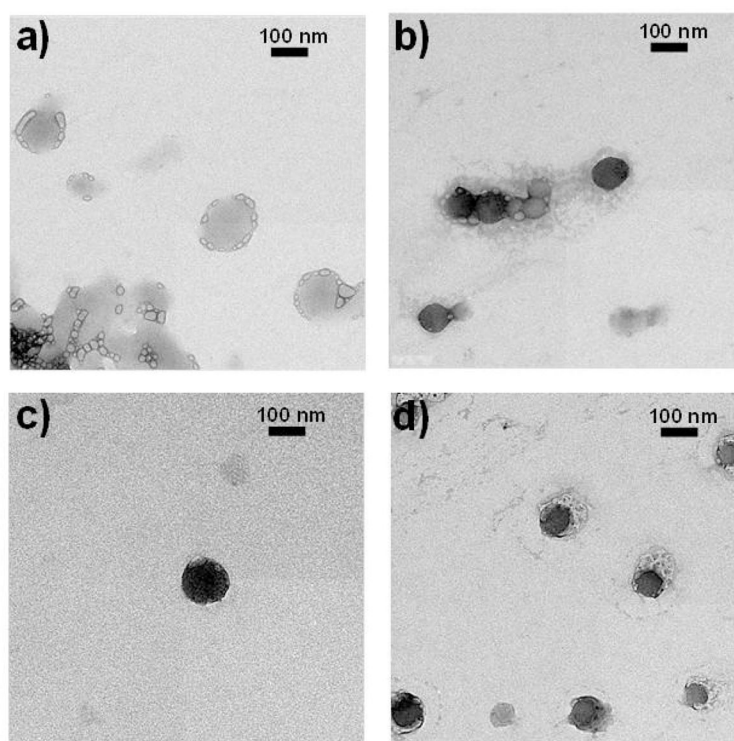


**Figure 3.** Silver carbene complex SCC23: a) chemical structure,<sup>20, 54</sup> and b) thermal ellipsoid plot with thermal ellipsoids shown at 50% probability.

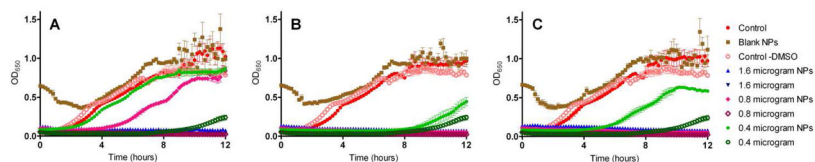




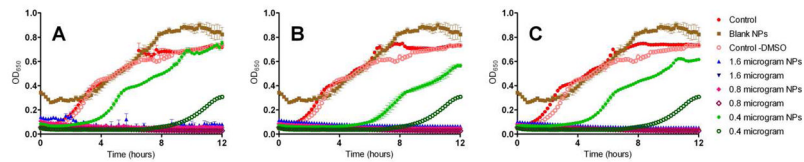
**Figure 4.** SCC23 encapsulation in the Ac-DEX particles (loading) compared to the initial feed of SCC23 used during particle formation. Loading and feeding are expressed in % SCC23 by weight / weight of Ac-DEX particle (for example: 10% SCC23 means that 10 mg of Ac-DEX particles contain 1 mg of SCC23).



**Figure 5.** TEM images of the Ac-DEX particles: a) empty Ac-DEX particles, size by TEM:  $140 \pm 40$  nm; b) Ac-DEX-SCC23-1 particles that contain about 6.0 % w/w SCC23, size by TEM:  $80 \pm 40$  nm; c) Ac-DEX-SCC23-2 particles that contain about 13.0 % w/w SCC23, size by TEM:  $100 \pm 40$  nm; d) Ac-DEX-SCC23-3 particles that contain about 15.4 % w/w SCC23, size by TEM:  $90 \pm 40$  nm.

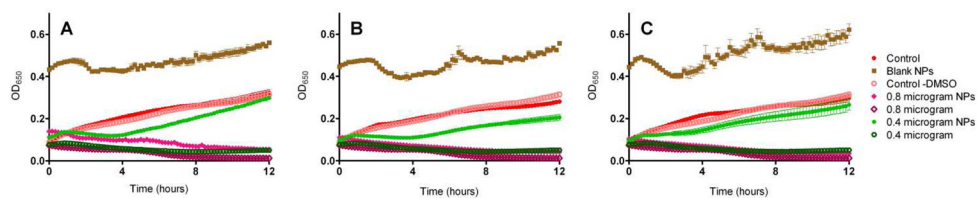


**Figure 6.** Comparison of the effect of increasing concentrations of SCC23 on the growth of a laboratory strain of *Pseudomonas aeruginosa* PAO1. The bacteria were exposed to SCC23 as a free drug or as SCC23 loaded Ac-DEX nanoparticle formulations. (A) Ac-DEX-SCC23-1 NPs (10% w/w), (B) Ac-DEX-SCC23-2 NPs (20% w/w), and (C) Ac-DEX-SCC23-3 NPs (30% w/w). Empty Ac-DEX NPs and M-H broth with and without 5% DMSO were used as controls for the experiment.



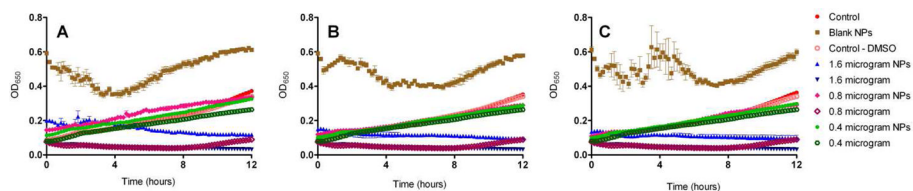
**Figure 7.**

Comparison of the effect of increasing concentrations of SCC23 on the growth of a clinical mucoid strain of *Pseudomonas aeruginosa* PA M57-15 isolated from a CF patient. The bacteria were exposed to SCC23 as a free drug or as SCC23 loaded Ac-DEX nanoparticle formulations. (A) Ac-DEX-SCC23-1 NPs (10% w/w), (B) Ac-DEX-SCC23-2 NPs (20% w/w), and (C) Ac-DEX-SCC23-3 NPs (30% w/w). Empty Ac-DEX NPs and M-H broth with and without 5% DMSO were used as controls for the experiment.

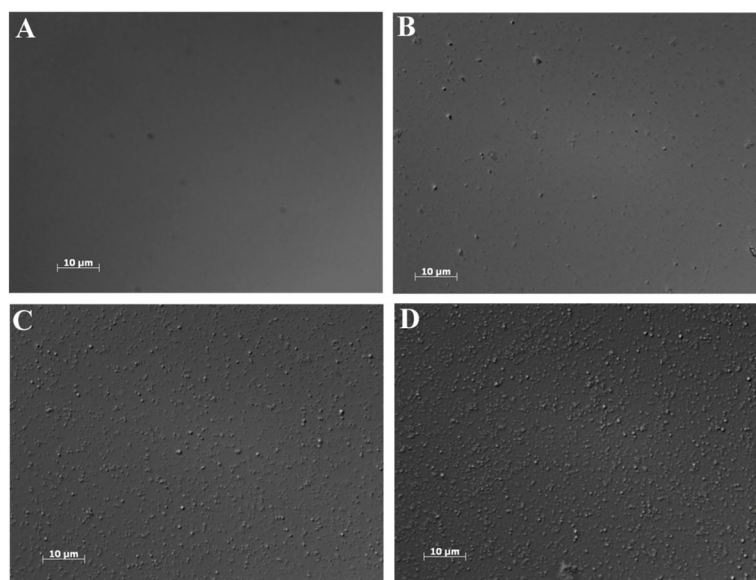


**Figure 8.**

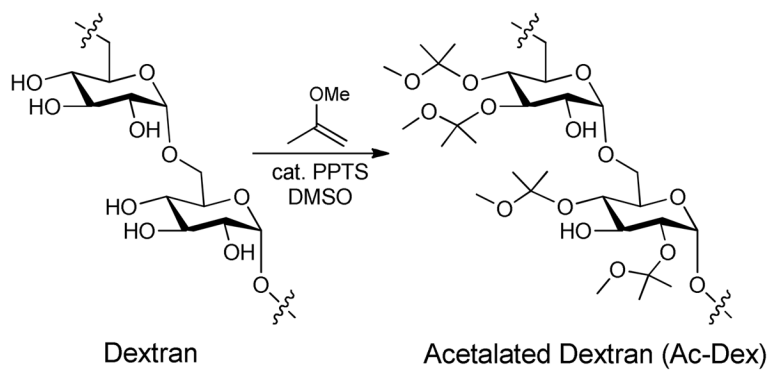
Comparison of the effect of increasing concentrations of SCC23 on the growth of a Methicillin-resistant *Staphylococcus aureus* strain SA LL06 isolated from a CF patient. The bacteria were exposed to SCC23 as a free drug or as SCC23 loaded Ac-DEX nanoparticle formulations. (A) Ac-DEX-SCC23-1 NPs (10% w/w), (B) Ac-DEX-SCC23-2 NPs (20% w/w), and (C) Ac-DEX-SCC23-3 NPs (30% w/w). Empty Ac-DEX NPs and M-H broth with and without 5% DMSO were used as controls for the experiment.



**Figure 9.** Comparison of the effect of increasing concentrations of SCC23 on the growth of a silver sensitive strain of *Escherichia coli* J53. The bacteria were exposed to SCC23 as a free drug or as SCC23 loaded Ac-DEX nanoparticle formulations. (A) Ac-DEX-SCC23-1 NPs (10% w/w), (B) Ac-DEX-SCC23-2 NPs (20% w/w), and (C) Ac-DEX-SCC23-3 NPs (30% w/w). Empty Ac-DEX NPs and M-H broth with and without 5% DMSO were used as controls for the experiment.



**Figure 10.** Optical microscopy images of Ac-DEX nanoparticles after nebulization obtained using a 100X objective. (A) phosphate buffer, (B) Ac-DEX-SCC23-1 NPs (10% w/w), (C) Ac-DEX-SCC23-2 NPs (20% w/w), and (D) Ac-DEX-SCC23-3 NPs (30% w/w).

**Scheme 1.**

Modification of Dextran with acetal groups yielding the Ac-DEX polymer.



**Table 1**  
SCC23 initial feed and final loading, and sizes of the Ac-DEX-SCC23 particles before and after lyophilization.

Ac-DEX Particles	Initial feed <sup>a</sup> % (w/w)	[Ag] <sup>b</sup> µg Ag per mg particle	[SCC23] <sup>c</sup> µg SCC23 per mg particle	Loading SCC23 % (w/ w)	Loading efficiency <sup>d</sup> %	Size after sonication <sup>e</sup> (nm)	Size after lyophilization <sup>f</sup> (nm)	Yield <sup>g</sup> %
Ac-DEX-SCC23-1	10	11	60	6.0	60	120 ± 40	110 ± 40	95
Ac-DEX-SCC23-2	20	24	130	13.0	65	140 ± 50	120 ± 50	85
Ac-DEX-SCC23-3	30	28	154	15.4	51	120 ± 40	120 ± 50	83
Ac-DEX-SCC23-4	40	30	165	16.5	41	100 ± 40	700 ± 200	81
Ac-DEX-SCC23-5	50	32	171	17.1	34	100 ± 40	700 ± 200	84

<sup>a</sup> Amount of SCC23 added to the Ac-DEX polymer prior to the particle formation.

<sup>b</sup> The concentration of silver was determined by ICP.

<sup>c</sup> The concentration of SCC23 was calculated taking in consideration the MW of SCC23 (585.25 g.mol<sup>-1</sup>) and the MW of silver (107.87 g.mol<sup>-1</sup>).

<sup>d</sup> The loading efficiency was calculated based on the initial feed and the final loading of SCC23.

<sup>e</sup> Size of the Ac-DEX particles measured by DLS just after the sonication procedure (average of three measurements).

<sup>f</sup> Size of the particles measured after centrifugation, washing, lyophilization and redispersion in PBS (average of three measurements).

<sup>g</sup> Yield was calculated based on the amount of Ac-DEX particles recovered after lyophilization.

Table 2

MIC and MBC comparison of Ac-DEX-SCC23 nanoparticle formulations. All MIC and MBC values for SCC23 in an encapsulated or free drug form and tobramycin in a free drug form are in  $\mu\text{g}/\text{mL}$ .

Bacteria	Ac-DEX-SCC23-1		Ac-DEX-SCC23-2		Ac-DEX-SCC23-3		Empty Ac-DEX		SCC23		Tobramycin	
	MIC	MBC	MIC	MBC	MIC	MBC	MIC	MBC	MIC	MBC	MIC	MBC
<i>Pseudomonas aeruginosa</i> (PA 01)	4	16	4	16	4	16	na	na	1	4	4	8
<i>Pseudomonas aeruginosa</i> (PA M57-15)	8	16	4	4	4	4	na	na	0.5	1	0.5	1
Methicillin-resistant <i>Staphylococcus aureus</i> (SA LL06)	4	16	4	16	4	8	na	na	2	4	>20	>20
<i>Escherichia coli</i> J53	4	4	4	8	4	4	na	na	1	1	1	1
<i>Escherichia coli</i> J53 + pMG101	32	32	16	16	16	16	na	na	6	8	1	1

Table 3

Comparison of growth inhibitory characteristics of various SCC23 loaded Ac-DEX nanoparticle formulations (X = no growth of bacteria, G = growth of bacteria).

SCC23 dose (µg/well)	Ac-DEX-SCC23-1	Ac-DEX-SCC23-2	Ac-DEX-SCC23-3	Empty Ac-DEX	Free SCC23
<i>Pseudomonas aeruginosa</i> (PA 01)					
6.4	X	X	X	G	X
3.2	X	X	X	G	X
1.6	X	X	X	G	X
0.8	G	X	X	G	X
0.4	G	G	G	G	G
<i>Pseudomonas aeruginosa</i> (PA M57-15)					
6.4	X	X	X	G	X
3.2	X	X	X	G	X
1.6	X	X	X	G	X
0.8	X	X	X	G	X
0.4	G	G	G	G	G
Medicillin-resistant <i>Staphylococcus aureus</i> (SA LL06)					
6.4	X	X	X	G	X
3.2	X	X	X	G	X
1.6	X	X	X	G	X
0.8	X	X	X	G	X
0.4	G	G	G	G	X
<i>Escherichia coli</i> 153					
6.4	X	X	X	G	X
3.2	X	X	X	G	X
1.6	X	X	X	G	X
0.8	G	G	G	G	G
0.4	G	G	G	G	G
<i>Escherichia coli</i> 153 + pMG101					
6.4	X	X	X	G	X

SCC23 dose ( $\mu\text{g}/\text{w}/\text{ell}$ )	Ac-DEX-SCC23-1	Ac-DEX-SCC23-2	Ac-DEX-SCC23-3	Empty Ac-DEX	Free SCC23
3.2	X	X	X	G	X
1.6	G	G	G	G	X
0.8	G	G	G	G	G
0.4	G	G	G	G	G